

## PREPARATION AND CHARACTERIZATION OF MAGNETIC ZnO/ferrite NPs FOR Cu<sup>2+</sup> REMOVAL FROM AQUEOUS SOLUTION

Sofien SAIDANI<sup>1,2,3</sup>, Lotfi BEN TAHAR<sup>2,3,4</sup>, Agnès SMITH<sup>1</sup>, Youssef EL HAFIANE<sup>1</sup>, Leila SMIRI<sup>2</sup>

<sup>1</sup>) *Université de Limoges, Institute of Research on Ceramics, IRCER - UMR 7315, Centre Européen de la Céramique, 12 rue Atlantis, 87068 Limoges cedex, France*

<sup>2</sup>) *University of Carthage, Laboratoire des composés hétéro-organiques et des matériaux nanostructurés-LR18 ES11, Faculty of Sciences of Bizerte, Jarzouna 7021, Tunisia*

<sup>3</sup>) *University of Tunis El Manar, Faculty of Sciences of Tunis, 2092 Tunis, Tunisia*

<sup>4</sup>) *University of Northern Border, College of Science of Arar, P.O. Box 1231, Arar 91431, Kingdom of Saudi Arabia*

**Abstract:** The increasing level of heavy metal ions in wastewater present a serious risk for human health and ecological system because they are non-biodegradable. Magnetically assisted chemical separation method using magnetic nanoparticles with a large active surface opens the door to a new generation of waste water treatment technology. In the present work, magnetic ZnO/ferrites nanoparticles were prepared to improve the efficiency of copper removal from artificial water. The ZnO/ferrites nanoparticles were synthesized by hydrothermal method and were characterized by several techniques. The adsorption properties as function of different parameters were carried out in order to understand the mechanism of adsorption.

**Keywords:** Waste water treatment, Magnetic nanoparticles.

### 1. INTRODUCTION

The presence of heavy metals in waste water (WW) becomes one of the most delicate problem for the environmental equilibrium [1]. The increasing level of heavy metal ions in wastewater presents a serious risk for human health and ecological system because they are non-biodegradable [2] [3]. Since the quantity of WW records a continuous increase [4] and new non-degradable pollutants, which are called “contaminants of emerging concern”, emerge as serious problems for water pollution [5], the conventional methods of WW treatment (coagulation–flocculation, chemical precipitation, adsorption, ion exchange, membrane filtration...) become insufficient to ensure the environmental protection [6]. The application of these methods becomes limited due to the presence of several problems such as the efficacy, the high demand for energy and the low selectivity [6]. Therefore, new WW treatment methods are required. Nowadays, nanotechnology is involved in various application areas: physical, chemical, biological and even in the field of environmental protection [7]. This progress coincides with the environmental intervention demands. Magnetically Assisted Chemical Separation (MACS) method using magnetic NPs with a large active surface opens the door to a new generation of wastewater treatment technology [8]. Ferrite magnetic NPs seem to be the most promoter type due the low-cost, the surface modifiability and the high recyclability [9].

Copper ion, which is an abundant and naturally present in wastewater, is one of heavy metals and can be harmful to human health [1]. Therefore, the removal of copper from wastewater becomes an important research topic, trying to improve the adsorption capacity and kinetic parameters and rich a good way to effectively remove Cu<sup>2+</sup>. Several methods have been adopted for the removal of copper ions from aqueous media. the most used techniques to remove the copper is chemical precipitation [10], ion exchange [11], electro-coagulation [12] and adsorption [13]. Several materials have been employed to adsorb copper from water and wastewater [13] [14] [15]. However, each adsorbent has some limitation in applications [16]. MACS technique of adsorption has been applied for the removal of copper ion from wastewater (artificial or not) [17] [18] [19].

In the present work, magnetic ZnO/ferrites NPs were synthesized to improve the efficiency of copper adsorption with the formation of highly active surface area. ZnO NPs were carried out using hydrothermal method in the

presence of ferrite NPs to ensure the assemblage between two compounds which was studied by several techniques. The adsorption of copper ions was tested in order to study the effect of the presence of ZnO particles.

## 2. PROCEDURE

### 2.1. Nanoparticles preparations

Magnetic-ferrite NPs, denoted as Magn, were produced by a chemical co-precipitation route. ZnO/ferrite NPs were prepared using Magn powder through hydrothermal method. Two type of ZnO/ferrite NPs were provided by varying the quantity of Magn NPs; high content and low content denoted as ZnO/Magn1 and ZnO/Magn2, respectively.

### 2.2. Solid-liquid Extraction procedure

Artificial  $\text{Cu}^{2+}$  contaminated solution was prepared for  $\text{Cu}^{2+}$  adsorption study. The initial concentration is fixed at  $100 \text{ mg.L}^{-1}$ . Solid-liquid extraction manipulation were performed by a mechanical shaker at 380 rpm with 10 mg of as-prepared dry magnetic adsorbent in contact with 10 mL of  $\text{Cu}^{2+}$  solution at  $25 \text{ }^\circ\text{C}$ . It was confirmed through the preliminary experiments that 120 min was enough to attain equilibrium between adsorbent and adsorbate for these three samples. For each adsorption measurement, the stirring was stopped, and the sorbent was separated by an external magnet. The residual metal concentration in the supernatant was determined using the UV-vis spectrophotometer with EDTA as a complexing agent. The wavelength was fixed at 735 nm, which corresponds to the maximum absorption of the  $\text{Cu}^{2+}$ -EDTA complex.

## 3. RÉSULTATS ET DISCUSSION

### 3.1. Phase formation

X-ray diffraction (XRD) was performed for the three samples to identify formed crystallographic phases. XRD patterns are presented in Fig. 1. The identification of diffraction patterns reveals the formation of spinel-type for Magn powder and the presence of both of spinel-type and wurtzite-type structure for ZnO/Magn powders. Magn sample presents very large peaks, which affirms the presence of very fine NPs. No peaks of any other phases are observed in particles XRD patterns, indicating the high purity of the products. The position and relative intensity of the diffraction peaks of Magn sample match well with the standard XRD data of maghemite. The formation of this structure can be due to the oxidation of  $\text{Fe}^{2+}$  ions due to the reactive surface of NPs [20]. Moreover, the diffraction peaks of ZnO/Magn sample reveal the presence of two structure; wurtzite-type structure and spinel structure, which shows a little displacement of diffraction peaks to the low angles compared to Magn sample as presented in fig. 1. This displacement is due to the increase of lattice parameters. This change can be related to the formation of franklinite, which has higher lattice volume than maghemite (Maghemite:  $8.34 \text{ \AA}$  [21], franklinite:  $8.44 \text{ \AA}$  [22]).

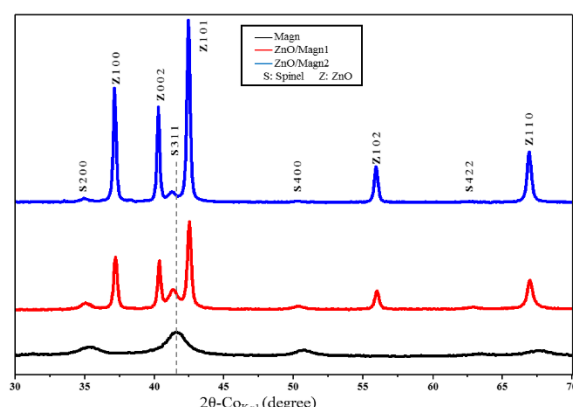


Fig.1: X-ray diffraction of different samples showing the presence of spinel and ZnO structure with the displacement to high angle of (311) spinel peak.

### 3.2. Microstructure

In order to investigate the microstructure of powder, samples were studied by transmission electronic microscope. TEM images of Magn particles show the presence of very fine particle with average size of 15 nm and near-spherical shape as presented in fig. 2-A. TEM images of ZnO/Magn2 show almost agglomerated NPs for all samples as presented in fig. 2-B. The morphology of ZnO/Magn2 NPs presents two populations, fine particles with rectangular shape, which resemble to Magn particles, and large particles with elongated shape as

presented in Fig. 2-B. To identify the nature of each population, the SAED of the two populations were provided in fig. 2. The SAED pattern of the zone-a (fine particles) shows that the diffraction rings are associated to polycrystalline spinel phase. The SAED pattern of zone-b (large particles) corresponds to single-crystal of the wurtzite structure along  $[1\bar{2}10]$ . These results are in accordance with identified phases from XRD results.

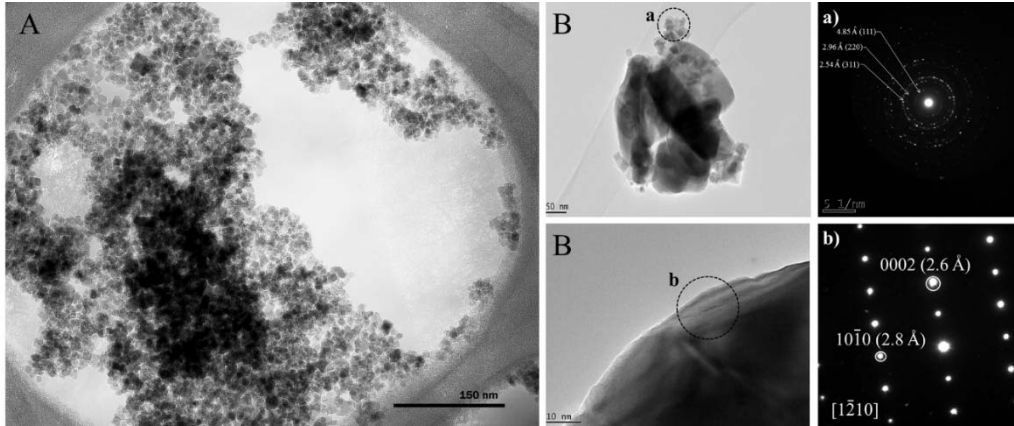


Fig. 2: A: TEM observation of Magn, B: ZnO/Magn2 nanoparticles with two selected area electron diffraction of two type of nanoparticles: zone (a) for fine particles which the diffraction rings are associated to spinel phase and zone (b) for large particles along  $[1\bar{2}10]$  orientation in the wurtzite phase.

### 3.3. Magnetic properties

Hysteresis loops revealed a superparamagnetic behavior of the NPs at 27 °C as presented in figure 3. In addition, as expected, the saturation magnetization of ZnO/ferrite NPs was found to be much lower than that of Magn NPs due to the diamagnetic character of ZnO.

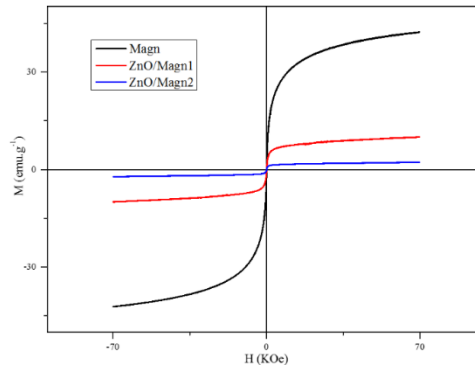


Fig. 3: Hysteresis loops of different samples at 27 °C.

### 3.4. Copper removal efficiency

The evolution of the uptake  $Q_t$  ( $\text{mg.g}^{-1}$ ) as a function of the time  $t$  (min) is plotted in figure 4. The uptake of Magn samples achieved  $43.2 \text{ mg.g}^{-1}$ . The addition of ZnO NPs promotes the adsorption of copper ions up to 91.73 and 92.02  $\text{mg.g}^{-1}$  for ZnO/Magn1 and ZnO/Magn2, respectively. In order to study kinetics properties of the adsorption mechanism, the pseudo-second-order and the pseudo-first-order equations were used to describe the phenomena. The first equation is often successfully used to describe the kinetics of the adsorption mechanism of metal ions on oxide adsorbent. In this case, the pseudo-second-order describes well the experimental results as presented in Figure-7. The equation 1 is expressed as follows:

$$\frac{dQ_e}{dt} = K_2(Q_e - Q_t)^2 \quad (1)$$

where  $K_2$  ( $\text{g} \cdot (\text{mg} \cdot \text{min})^{-1}$ ) is the second-order rate constant,  $Q_e$  ( $\text{mg.g}^{-1}$ ) is the amount of adsorbed metal ions and  $Q_t$  ( $\text{mg.g}^{-1}$ ) gives the adsorbed amount of  $\text{Cu}^{2+}$  at any time  $t$  (min). The equation 1 can be integrated for the boundary conditions  $t = 0$  ( $Q_t = 0$ ) to  $t = t_e$  ( $Q_t = Q_e$ ) and then liberalized; this leads to:

$$\frac{t}{Q_t} = \frac{1}{K_2 Q_e^2} + \frac{t}{Q_e} \quad (2)$$

By plotting  $\frac{t}{Q_t}$  versus  $t$  in figure 9, a straight line is obtained with the slope of  $\frac{1}{K_2 Q_e^2}$  and intercept of  $\frac{1}{Q_e}$ . The high correlation coefficient indicates the applicability of the pseudo second-order model and adsorption follows the

chemisorption mechanism. Pseudo-first-order mode was also tested to describe the kinetics of the adsorption process. The low values of correlation coefficient ( $R^2 < 0.90$ ) indicated that they were not suitable for explanation of adsorption mechanism.

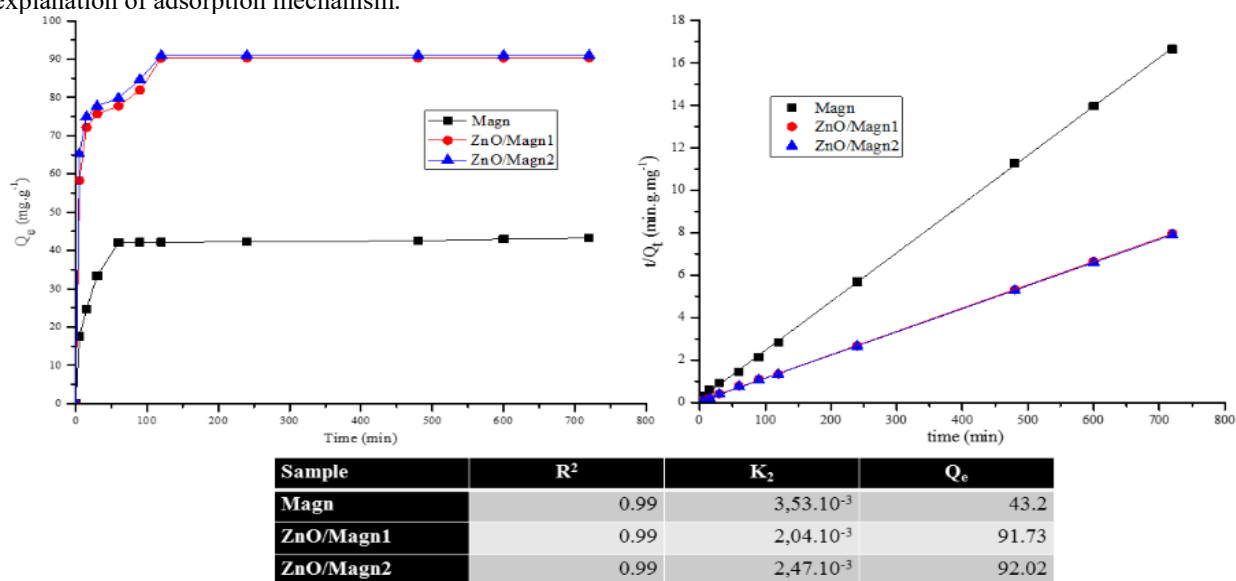


Fig. 4: Kinetic study of the adsorption of  $\text{Cu}^{2+}$ . On the left side is presented the evolution of the uptake as a function of the time for different samples. On the right side is plotted the validation of the pseudo-second-order model.

#### 4. CONCLUSION

Besides the high particle size of ZnO NPs compared to ferrites NPs, its presence promotes the adsorption ability of  $\text{Cu}^{2+}$  and thus the removal of copper ions from water. This result can be due to ZnO surface properties, which seems to be more adequate for  $\text{Cu}^{2+}$  adsorption than ferrite surface. Besides, the presence of ZnO NPs affects the magnetic properties of powder and thus the separation performance. Therefore, the quantity of ZnO NPs should be adjusted to optimize both of properties; adsorption capacity and separation efficiency.

#### REFERENCES

- [1] I. Sá, M. Semedo, et M. E. Cunha, Porto Biomed., 2016.
- [2] G. Tepanosyan, L. Sahakyan, O. Belyaeva, N. Maghakyan, et A. Saghatlyan, Chemosphere, 2017.
- [3] V. Vella, R. Malaguarnera, R. Lappano, M. Maggiolini, et A. Belfiore, Mol. Cell. Endocrinol., 2017.
- [4] D. Ficaí, A. Ficaí, et E. Andronescu, A. M. Grumezescu, Éd. Academic Press, 2017.
- [5] M. O. Barbosa, N. F. F. Moreira, A. R. Ribeiro, M. F. R. Pereira, et A. M. T. Silva, Water Res., 2016.
- [6] K. R. Kunduru, M. Nazarkovsky, S. Farah, R. P. Pawar, A. Basu, et A. J. Domb, Water Purification, 2017.
- [7] L. Farzin, M. Shamsipur, et S. Sheibani, Talanta, 2017.
- [8] L. B. Tahar, M. H. Oueslati, et M. J. A. Abualreish, J. Colloid Interface Sci., 2018.
- [9] I. Ali, Chem. Rev., 2012.
- [10] J.-Y. Choi, D.-S. Kim, et J.-Y. Lim, J. Environ. Sci. Health Part A., 2006.
- [11] Y. Chen, B. Pan, H. Li, W. Zhang, L. Lv, et J. Wu, Environ. Sci. Technol., 2010.
- [12] F. Akbal et S. Camcı, Desalination, mars 2011.
- [13] T. Vengris, R. Binkienė, et A. Sveikauskaitė, Appl. Clay Sci., 2001.
- [14] W. S. Wan Ngah et M. A. K. M. Hanafiah, Bioresour. Technol., 2008.
- [15] S. S. Ahluwalia et D. Goyal, Bioresour. Technol., 2007.
- [16] D. Mohan et C. U. Pittman, J. Hazard. Mater., 2007.
- [17] Y.-M. Hao, C. Man, et Z.-B. Hu, J. Hazard. Mater., 2010.
- [18] X. Liu, Q. Hu, Z. Fang, X. Zhang, et B. Zhang, Langmuir, 2009.
- [19] Y.-T. Zhou, H.-L. Nie, C. Branford-White, Z.-Y. He, et L.-M. Zhu, J. Colloid Interface Sci., 2009.
- [20] K. Haneda et A. Morrish, J. Phys. Colloq., 1977.
- [21] A. N. Shmakov, G. N. Kryukova, S. V. Tsybulya, A. L. Chuvilin, et L. P. Solovyeva, J. Appl. Crystallogr., 1995.
- [22] Alessandro Pavese, Davide Levy et Andreas Hoser, American Mineralogist, 2015.